MULTI-SCALE MODELING OF ADDITIVE MANUFACTURING PROCESS

SHUBHAM CHANDRA[a],
GANDHAM PHANIKUMAR[b], GIM LEE SEET[a], SHU BENG TOR[a], CHEE KAI CHUA[a]

[a] *Singapore Centre for 3D Printing, School of Mechanical and Aerospace Engineering, Nanyang Technological University, 50 Nanyang Avenue, Singapore - 639798*

[b] *ICME Laboratory, Department of Materials and Metallurgical Engineering, Indian Institute of Technology Madras, Chennai, Tamil Nadu - 600036, India*

ABSTRACT: Additive manufacturing techniques, specifically those currently employed in metal-based manufacturing; involve heat transfer and fluid flow physics which are far too complex to be covered in an analytical form. This limits the control over material microstructure thus obtained in a deposited alloy component. To this need, a multi-scale numerical study is carried out combining a three-dimensional finite element (FE) based macro-scale and a cellular automaton (CA) based meso-scale model in order to simulate the dendritic grain growth in the selective laser melting (SLM) technique. The macro-scale model successfully simulates the heat transfer and fluid flow physics associated with a moving melt pool. The CA model deals with the phenomena of solute-diffusion on a meso-scale during solidification. The thermal coupling between the two length scales results in a reasonably accurate model capable of accounting for steep thermal gradients, large cooling rates and complex thermal cycles associated with the solidification phenomena occurring during laser-based manufacturing process.

KEYWORDS: Additive Manufacturing, Numerical Modeling, Cellular Automata

INTRODUCTION

Additive manufacturing (AM), derived from 3D printing, is the technique of material addition, preferably metal powder, on to a substrate in the presence of a heat source which carries out layer-wise thermal bonding of the metal powder resulting in a final deposited component. It is a process that involves high rates of cooling and steep thermal gradients which affect the microstructure of the resultant part. Thus, a proper understanding of the physics associated with it and a predictive capability over the microstructure obtained is crucial in enabling AM to establish itself as a major mode of component production. The current study focuses on the development of a multi-scale numerical model of a laser-based manufacturing process where the macro-scale simulation of material melting/solidification and fluid flow in the melt pool in the presence of high power source is carried out using nonlinear finite element method (FEM) and the meso-scale simulation of the grain growth during solidification of the melt pool is carried out using cellular automaton finite difference CAFD method.

Proc. of the 2nd Intl. Conf. on Progress in Additive Manufacturing
Edited by Chee Kai Chua, Wai Yee Yeong, Ming Jen Tan, Erjia Liu and Shu Beng Tor

Published by Research Publishing, Singapore
ISSN: 2424-8967

Earlier work by Yin and Felicelli (2010) utilized a similar FE-CA coupling of multiscale phenomena associated with the laser engineered net shaping (LENS) process. This work remains one of the first multiscale numerical studies of additive manufacturing carried out successfully capturing the dendritic grain growth phenomena in the melt pool. However, it was confined to a two-dimensional heat transfer simulation of the process both on a macro- and micro-scale thus entirely neglecting the heat transfer in the direction perpendicular to laser scanning and fluid flow in the melt pool.

The current study is focused on the development of a multi-scale numerical model for the laser based manufacture and repair process. The simulation has been carried out for a binary alloy AB4 for general laser process parameters specifically, with a successful implementation of general double ellipsoidal heat source model (Goldak, Chakravarti et al. (1984)).

MACRO-SCALE MODEL

In the present work, a three-dimensional modeling of the laser scanning process has been carried out using nonlinear FE package - COMSOL. The implication of this being that the phenomena of powder addition (as in LENS) or melting on the powder bed (SLM) has not been considered. The computational domain is a block of length 20mm, width 10mm and height 5mm with a symmetry boundary condition applied across the melt pool width. The governing mass, momentum and energy conservation equations employed using COMSOL in the study can be written as:

Mass Conservation Equation
The general form of mass conservation equation is given as:

$$\frac{\partial \rho}{\partial t}+\nabla.(\rho \mathbf{u}) = 0 \tag{1}$$

where, ρ is the density of the fluid and $\boldsymbol{u}$ the velocity field in the domain.

For incompressible fluids, this equation simplifies as:

$$\nabla.\mathbf{u}=0 \tag{2}$$

Momentum Conservation Equation
The momentum conservation equation in its general form is given as:

$$\frac{\rho \partial \mathbf{u}}{\partial t}+\rho \mathbf{u}\nabla.\mathbf{u}=\nabla.\left[-p\mathbf{I}+\mu\left(\nabla \mathbf{u}+(\nabla \mathbf{u}^{T})\right)-\frac{2}{3}\mu(\nabla.\mathbf{u})\mathbf{I}\right]+\mathbf{F} \tag{3}$$

where, p is the pressure, $\boldsymbol{F}$ the body force vector and μ the coefficient of dynamic viscosity.

Energy Conservation Equation
The general enthalpy equation can be written in the form:

$$\rho C_p \frac{\partial T}{\partial t}+\rho \mathbf{u}.\nabla T=\nabla.(k\nabla T)+Q \tag{4}$$

where, C_p is the specific heat capacity and Q the volumetric heat source.

The phenomena of melting/solidification due to the presence of heat source is accounted by taking the averaged values of the parameters in Eq. 4 as discussed briefly in work by Loh, Chua et al. (2015).

In Eq. 3, the body force vector is taken as the force of buoyancy under Boussinesq's approximation and the value of coefficient of dynamic viscosity is given as a function of temperature with distinct variation between solid and liquid phases.

In Eq. 4, a double ellipsoidal heat source model given by Goldak, Chakravarti et al. (1984) is used as volumetric heat source which is given as:

$$Q(x,y,z,t)=\frac{6\sqrt{3}f_f P}{abc\pi\sqrt{\pi}} e^{-\frac{3(x-x_1)^2}{a_1^2}} e^{-\frac{3(y-y_0)^2}{b^2}} e^{-\frac{3(z-z_0)^2}{c^2}} \quad \text{for, } x > x_1 \tag{5}$$

$$Q(x,y,z,t)=\frac{6\sqrt{3}f_r P}{abc\pi\sqrt{\pi}} e^{-\frac{3(x-x_1)^2}{a_2^2}} e^{-\frac{3(y-y_0)^2}{b^2}} e^{-\frac{3(z-z_0)^2}{c^2}} \quad \text{for, } x \leq x_1 \tag{6}$$

where, *P* is the power rating of heat source and *a, b, c* are the semi-axes of the heat source parallel to x, y and z directions respectively.

Boundary Conditions

Following heat transfer and fluid flow boundary conditions were applied at different x, y and z locations of the domain shown in Figure 1:

Heat Transfer Boundary Conditions

$-\mathbf{n}.(k\nabla T)=0$	Symmetry boundary condition	at y = 0
$-\mathbf{n}.(k\nabla T)=0$	Insulated boundary condition	at z = 0
$q= -h(T-T_0)- \sigma\epsilon(T^4-T_0^4)$	Heat flux boundary condition	at x = 0; x = 20; y = 10; z = 5

Fluid Flow Boundary Conditions

$\mathbf{u}.\mathbf{n}=0$	Symmetry boundary condition	at y = 0
$\mathbf{u}=0$	No slip boundary condition	at x = 0; x = 20; y = 10; z = 0

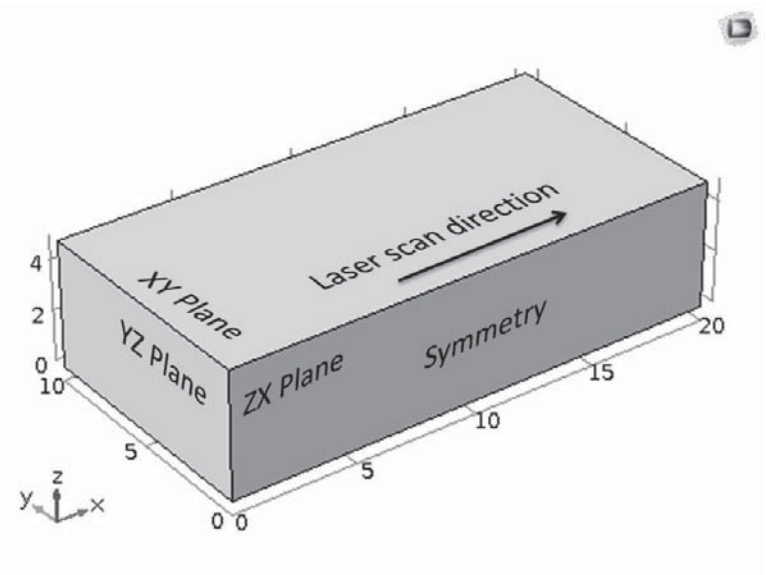

Figure 1. Macro-scale model with laser direction and planes chosen for 2D mesoscale modeling

Apart from these, Marangoni convection boundary convection was defined at z = 5mm.

MESO-SCALE MODEL

The meso-scale modeling of grain growth in melt pool was carried out using an open source code µMatIC (Lee, Chirazi et al. (2004)) which utilizes a modified version of decentered square/octahedron CA technique, given by Gandin and Rappaz (1997), in order to simulate the solute diffusion during solidification of a binary alloy melt. The solute diffusion is calculated via a difference solution of Fick's law:

$$\frac{\partial}{\partial t}\left(\rho_l C_l f_l + \rho_s C_s f_s\right) = \nabla.\left(\rho_l D_e \nabla C_l\right) + S \quad (7)$$

where, C is the solute concentration in solid and liquid phases denoted by subscripts s and l respectively, f is the fraction of phase and D_e is the effective diffusivity averaged over the phases.

The meso-scale simulations were carried out in two dimensions but in three different planes: XY, YZ and ZX planes as shown in Figure 1. The resultant thermal gradient obtained from the macro-scale model was supplied to the meso-scale model along with the slope of gradient magnitude.

RESULTS AND DISCUSSION

The macro-scale thermal history data was recorded at four points A, B, C and D having x, y and z coordinate specification of 10, 0, 5; 10, 0.5, 5; 9.7, 0, 5; and 10, 0, 4.7 respectively. In reference to Figure 1, this means that points A, C and D lie in the ZX plane and point B was taken in XY plane along the probable width of the melt pool.

Figure 2 shows the temperature variation with time recorded at aforementioned points of study. It is evident from the plot that the material at point B did not reach the melting temperature hence implying that the melt pool width is well below 1mm in the current study.

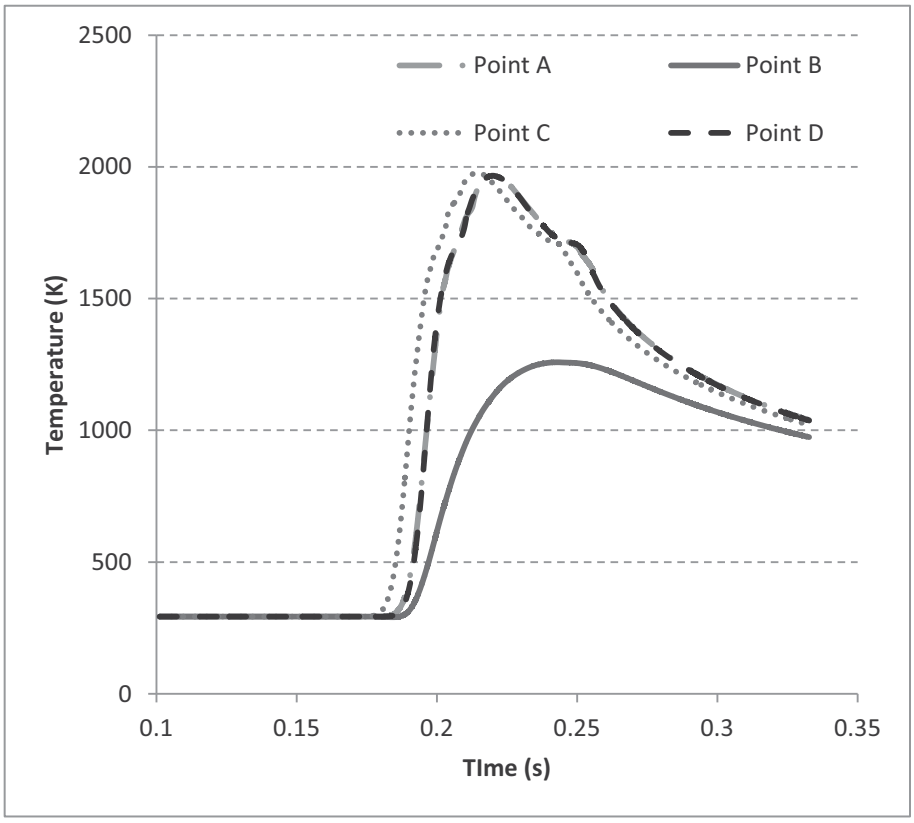

Figure 2. Thermal history plot at points A, B, C and D

It should also be noted that the thermal history curve at point A on the melt pool surface coincides almost completely with that at point D which is at a depth of 0.3mm from point A in the melt pool. A definitive conclusion can be made here that in comparison to the thermal gradients in x and y directions, which cause substantial temperature change along their respective axes, the thermal gradient along z direction remains dormant. Quantitatively, it was found out that near the interface, at point D, the thermal gradient in z direction was approximately 4 times less than that in x and y directions. This data was fed into the meso-scale CAFD model to visualize the grain growth in different planes within the melt pool.

The meso-scale simulations were carried out with a domain size of 0.3mm width and 0.3mm height. Figure 3 shows the simulation of dendritic growth at point D in a) xy; b) yz; and c) zx planes respectively. The simulations were carried out with fixed nucleation of 20 grains on the bottom wall of the domain with random variation in their orientation (from 20 to 60 degrees). Though the number of nucleation is too less to be practical, it gives a clear representation of the

competitive grain growth behavior with varying temperature gradient magnitude and direction. Figure 3 also consists of contour diagrams of thermal variation in each of the planes. The images shown below were taken for a simulation time of 0.04 seconds post-nucleation.

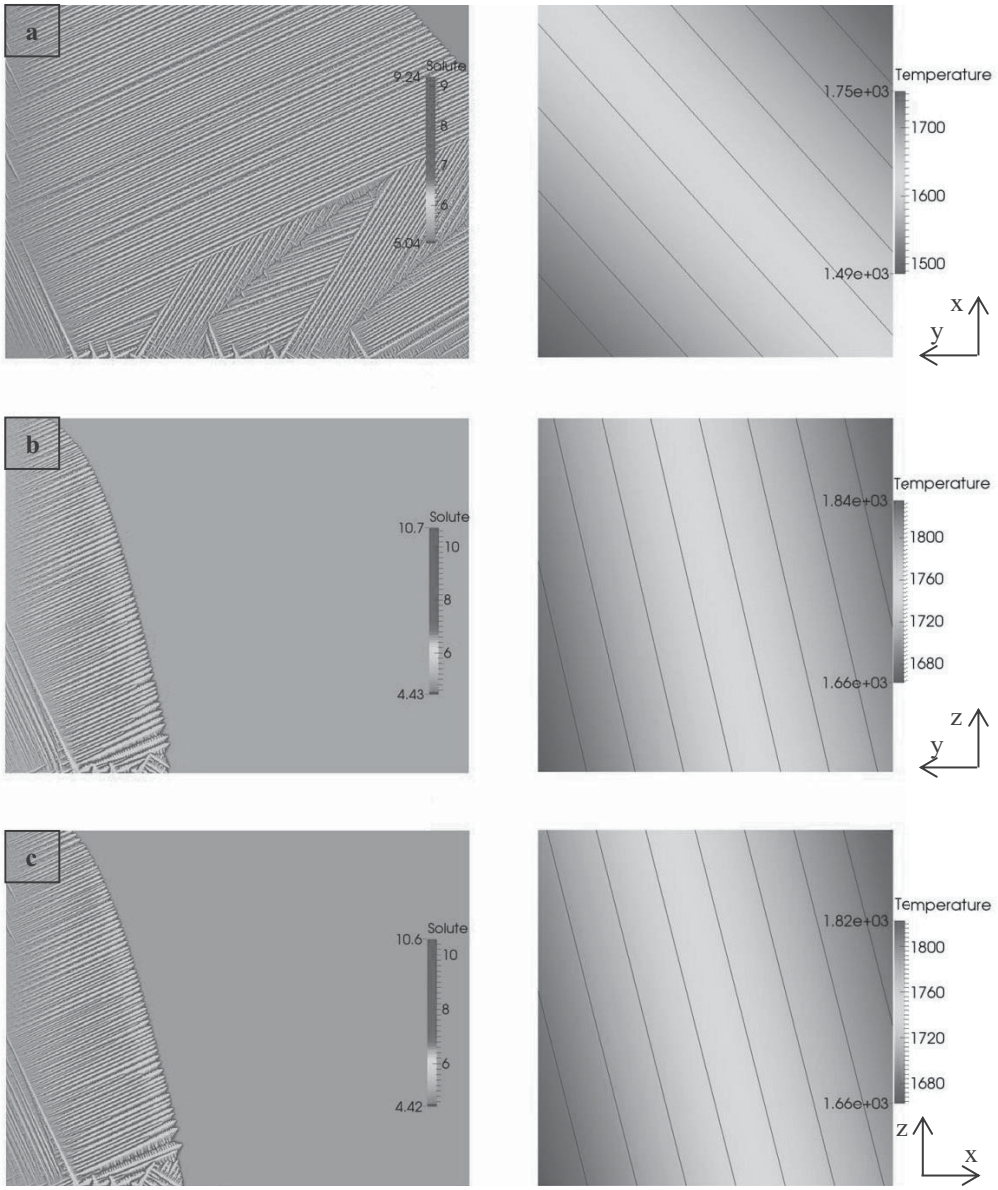

Figure 3. Grain growth simulation and temperature variation in the melt pool 0.04 seconds after nucleation in a) xy; b) yz; and, c) zx planes respectively

CONCLUSION

In the current study, a successful coupling of an FE-based macro-scale model was carried out with a meso-scale CAFD model. The macro-scale model is capable of covering the complex heat transfer and fluid flow physics involved in a laser processing technique without the phenomena of mass addition. The meso-scale model is also capable enough to account for the directional variation of thermal gradient within the melt pool and the phenomena of solute diffusion in a binary alloy.

The results from macro model clearly indicate that the dominating temperature gradient acting in the melt pool depends clearly on the processing conditions (insulated bottom of the base plate clearly has a detrimental effect on thermal gradient in the z-direction) and is varying within the melt pool as well. These effects will be accounted for any of the future works to be conducted.

The meso-scale simulation results show the grain growth variation in the different planes of the melt pool. They also reflect the competitive grain growth behavior clearly observed in rapid solidification conditions. Though the limitation of the present meso-scale model is clearly its application being confined to binary alloys, the future scope definitely involves extending the current model to multicomponent alloys.

The technique of laser processing involves varying heat transfer and cooling rates with the location of heat source, thus creating a geometry dependent non-uniformity in the microstructure obtained in laser processed parts. Hence, this study is an initial step towards quantifying grain growth in the melt pool of a laser which as observed varies with x, y and z directions. The physical implementation of this model along with experimental validation will benefit in the prediction of final microstructure obtained in a component obtained from an AM process.

ACKNOWLEDGEMENTS

The authors are thankful to GE India Technology Centre Pvt. Ltd., Bangalore, India for a grant from GE Global Research for part of the work carried out at IIT Madras. Authors sincerely acknowledge Dr. Anirban Bhattacharya for his guidance and never-ending support in meso-scale modeling which has been a major means of propulsion for this work to this breadth.

APPENDIX

Parameters employed for laser scanning

Laser power, P	=	4000 W
Scan speed, v	=	50 mm/s
Stefan's constant, σ	=	5.67×10^{-8} W m^{-2} K^{-4}
Emissivity, ε	=	0.8
Solidus temperature	=	1673K
Liquidus temperature	=	1723K

Heat source parameters

x_1	=	v x t mm
y_0	=	0
z_0	=	5 mm

Semi-axis for first half of heat source in x-direction, a_1	=	0.5 mm
Semi-axis for rear half of heat source in x-direction, a_2	=	2 mm
Semi-axis in y direction, b	=	0.5 mm
Semi-axis in z direction, c	=	10 mm

REFERENCES

Gandin, C. A. and M. Rappaz (1997). *A 3D Cellular Automaton algorithm for the prediction of dendritic grain growth*. Acta Materialia **45**(5): 2187-2195.

Goldak, J., A. Chakravarti and M. Bibby (1984). *New Finite Element Model for Welding Heat Sources.* Metallurgical transactions B **15 B**(2): 299-305.

Lee, P. D., A. Chirazi, R. C. Atwood and W. Wang (2004). *Multiscale modelling of solidification microstructures, including microsegregation and microporosity, in an Al–Si–Cu alloy*. Materials Science and Engineering: A **365**(1-2): 57-65.

Loh, L.-E., C.-K. Chua, W.-Y. Yeong, J. Song, M. Mapar, S.-L. Sing, Z.-H. Liu and D.-Q. Zhang (2015). *Numerical investigation and an effective modelling on the Selective Laser Melting (SLM) process with aluminium alloy 6061*. International Journal of Heat and Mass Transfer **80**: 288-300.

Yin, H. and S. D. Felicelli (2010). *Dendrite growth simulation during solidification in the LENS process.* Acta Materialia **58**(4): 1455-1465.